Electronic processes in polyaniline films photoexcited with picosecond laser pulses: A three-dimensional model for conducting polymers

I. A. Misurkin
Karpov Institute of Physical Chemistry, 103064 Moscow K-64, ulica Obukha 10, Russia

T. S. Zhuravleva and V. M. Geskin
Institute of Chemical Physics of the Russian Academy of Sciences, 117334 Moscow, Russia

V. Gulbinas, S. Pakalnis, and V. Butvilos
Institute of Physics, Lithuanian Academy of Sciences, 232053 Vilnius, Lithuania
(Received 23 February 1993; revised manuscript received 25 October 1993)

Photoinduced absorption data for polyaniline films in two forms, emeraldine base (EB) and emeraldine salt (ES), are presented and discussed. Electrochemically synthesized films were excited with laser pulses of large intensity (the energy $\simeq 2$ eV, the pulse duration $\simeq 8$ ps, the pulse energy up to 10 mJ/cm^2). Optical spectra of the EB and ES films in the temperature range from 298 to 363 K are also studied. The polymer film is presumed to be a three-dimensional (3D) system of long finite conjugated fragments of polymer chains. Considering each fragment integrally and taking into account the electronic polarization energy ($\simeq 1.5$ eV) for a charge in the film, the 3D model of a charge-transfer exciton is proposed. The low-energy absorption of EB and ES and the electronc processes in photoexcited films are interpreted within the framework of the proposed model, avoiding the commonly adopted approach of an isolated polymer chain.

I. INTRODUCTION

Conducting polymers, especially polyaniline (PANi), have recently attracted considerable attention because of the interesting properties of these materials. In recent years, a number of papers have been published (see, for example, Ref. 1) where the photoinduced absorption (time-resolved excitation spectroscopy) measurements of different forms of PANi (Fig. 1) were discussed. Usually the emeraldine-base (EB) form of PANi, synthesized chemically, is investigated using either the excitation pulses of a low intensity laser (the energy density of a pulse $P \simeq 10^{-3}$ mJ/cm^2) in the ps and ns time ranges or with the help of a steady-state Ar^+ laser with a mechanical chopper. Investigations of the photoinduced infrared (IR) (Refs. 2–6) and ultraviolet (UV) (Refs. 3, 5, 7–11) spectra of EB gave an insight into physical phenomena observed in the photoinduced polymer material. Kim and co-workers[2,3,9] found that the photoinduced absorption spectra of EB in IR and UV regions are very similar to the nonexcited absorption spectra of the emeraldine-salt (ES) form of PANi. Based on this similarity, the authors[2,3,9] concluded that the photoexcitation of EB by photons with energy from 2 to 2.5 eV produces the charged species, which are usually generated through protonation of EB. Long-lived states with unpaired electrons detected after photoexcitation of EB (Refs. 8 and 9) and photoconductivity measurements of EB (Refs. 4, 9, and 12) also indicate that the photoexcitation produces charged species. It was also found that charge carriers are produced by direct optical transitions.[12] Roe *et al.*[11] reported the existence of two distinct decay mechanisms for recombination of photoexcited states in EB: the temperature (T) independent (dispersive) decay of the photoinduced bleaching $\simeq t^{-0.11}$ for short times (40 ps $< t <$ 4 ns) and long-time photoinduced bleaching (from 1 ms to 10 min) which varies as $t^{-\beta}$ and is weakly T dependent ($\beta \simeq 0.5$ at 200–300 K and $\simeq 0.4$ at 15 K).

In the interpretation of the results of photoexcitation experiments for EB and other forms of PANi (leucoemeraldine base [LB], pernigraniline base [PNB]), the central roles have been assigned to phenyl-ring rotations with creation of massive polarons bound to these rings.[5,11–15] It was suggested[9,12] that the photoexcitation transferred an electron into a flat excited-state band, which is localized on the rings, and the hole, resting in the occupied band, provided the photocurrent along the polymer chain. A model was also proposed to account for photocreation of defect states in LB and EB including the charge transfer from one part of a polymer chain to another, and it was suggested that the long-lived excitations were stabilized by ring rotations and solid-state constraints that inhibit ring relaxation to the initial conformation.[5,11] Nevertheless, the appearance of separated charges in the polymer sample after absorption of one photon with energy $\simeq 2$ eV attracts particular interest as an unsolved problem.

We believe that the difficulties in explaining many unusual phenomena in conducting polymers arise mainly from the commonly adopted approximation of an isolated polymer chain. The main difficulty results from the necessity to explain the electrophysical properties of conducting polymers only by single polymer chain features. This approach found wide use in explaining the electro-

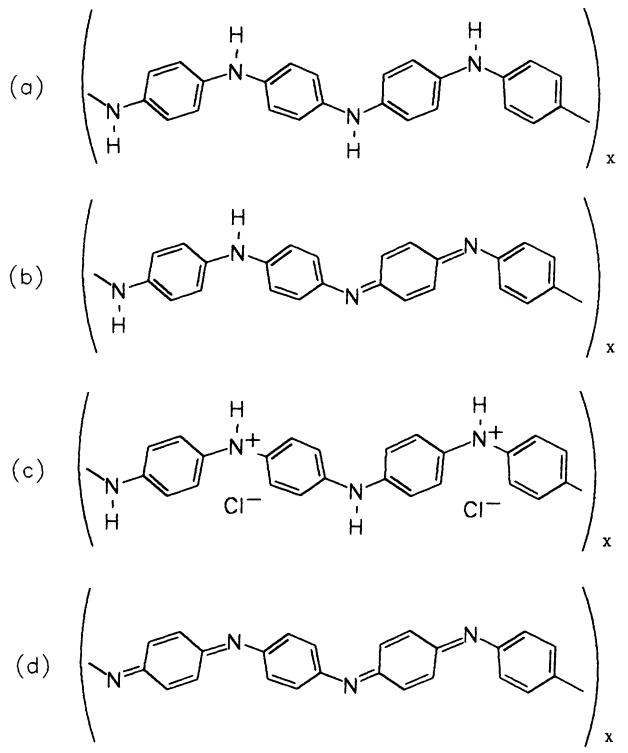

FIG. 1. Idealized repeat structure for (a) leucoemeraldine base, (b) emeraldine base, (c) emeraldine salt, and (d) pernigraniline base.

physical properties of polyacetylene, polydiacetylene, polythiophene, and other polymers with conjugation in the main chain.[16] Meanwhile, only a little attention is currently paid to an important feature of the real structure of these materials. Namely, polymeric materials consist of bundles of chains arranged parallel to each other. Distances between the neighbor chains are rather small: $\simeq 4.3$ Å in polyacetylene,[17] $\simeq 4.85$ Å in PANi.[18] Such distances make electron hopping between neighbor chains easy. In addition, the full conjugation is broken, and the polymer chains are divided by the chain defects into conjugated fragments (CF) of a finite length. This fact does allow us to speak about the average length of conjugation which is essentially the average length of these CF's. Moreover, it is impossible to imagine charge transport (electrical current) in a CF of an isolated chain, because the mean value of the radius vector of an electron in any of the electron states of the CF coincides with the middle of the fragment. Because of this, one may only consider the charge transfer on a bundle of chains between neighbor CF's taken as a whole. For these reasons we suggest that a conducting polymer should be considered as a three-dimensional (3D) system of long finite CF's. An interpretation of the experimental data for polyacetylene based on these concepts has been developed recently.[19–21] Analyzing the results of conductivity, thermopower, and dielectric-constant studies, Wang *et al.*[22] also concluded that the metallic states of the ES form of PANi are essentially 3D states and ES is composed of bundles of coupled parallel chains instead of isolated chains. These results emphasize the importance of interchain coupling in avoiding 1D electron localization in conducting polymers.[22]

Many properties of conducting polymers are rather similar, even though these polymers are chemically different. Among these properties one can point to the value of the energy $\Delta E_1 \simeq 2$–2.5 eV of the first intense maximum in an optical spectrum and the typical changes in optical-absorption spectra and conductivity, which accompany chemical doping or photoexcitation, etc.[1] The approach to describing the electrophysical properties of polyacetylene[19–21] is suitable for conducting polymers with a different chemical structure, because it takes into account only the basic parameters common to all polymers. These parameters are the average length of CF's, the electron affinity, and the ionization potential of an isolated CF, the parameter of the electron hopping between the neighbor CF's on neighbor chains, the polarization energy of all other CF's in the Coulomb field of a given charged CF or a charged defect, the energy of the first electronic excitation (ΔE_1) of an isolated CF, etc. The values of these parameters are usually nearly the same for all conducting polymers, and this fact explains the similarity of their properties.

In this paper, we present the results of the photoinduced-absorption measurements performed with the EB films. Photoexcitation was provided by means of high-intensity laser pulses (the energy $\simeq 2$ eV, the pulse duration $\simeq 8$ ps, and the energy density of the pulse mounted up to 10 mJ/cm^2). We were interested in the specific effects of a powerful laser pulse upon EB as well as new information on the photoelectronic processes in this form of PANi. The optical spectra of the EB and ES films have also been measured at different temperatures in the range from 298 to 363 K to allow for the effect of the sample heating caused by an intense pulse on the optical spectra. Discussing our experimental data in terms of the above-mentioned approach,[19–21] we argue that PANi represents a 3D system of long finite CF's of polymer chains. Furthermore, we propose a 3D model of a localized exciton with an electron transfer to a number of CF's. Finally, we suggest a new interpretation of the low-energy absorption and of the electronic processes in the photoexcited films based on this model of the charge-transfer exciton.

II. EXPERIMENT

The polyaniline ES films were deposited by the electrochemical techniques[23] [galvanostatically or by cycling the potential of the electrode from -0.2 to $+0.79$ V vs the saturated calomel electrode and using a nonstirred aqueous solution of H_2SO_4 ($1.0M$) and aniline (freshly distilled, $0.4M$)] onto tin oxide (SnO_2) glass substrates. The film thicknesses, ranging from 0.1 to 0.2 μm, were estimated.[24–26] The PANi-ES film was transformed to the EB form by keeping it in ammonia vapor for several minutes.

The direct absorption spectra were measured with a Perkin-Elmer UV/Vis spectrophotometer in the range of 350–900 nm (using a diffuse reflection chamber) and

Shimadzu UV-365 spectrophotometer in the range of 200–2500 nm.

The time-resolved photoinduced-absorption measurements were carried out in the standard pump-and-probe configuration. For the kinetic measurements, the second harmonic ($\lambda_{excit}=590$ nm, $\simeq 2.1$ eV) of the Stokes's component of a $KGd(WO_4)_2:Nd^{3+}$ laser[27] was used (pulse length 5 ps, repetition rate 3 Hz). A parametric generator of light was the probe source. The energy of the excitation pulses varied from 1 to 10 mJ/cm^2. Photoinduced-absorption spectra were obtained with the help of a YAG:Nd^{3+} laser (where YAG denotes yttrium aluminum garnet) (pulse length 5 ps, repetition rate 3 Hz). The second harmonic of a parametric generator ($\lambda_{excit}=590$ nm, $\simeq 2.1$ eV) was used as a pump source. The picosecond continuum generated in heavy water was used as a probe source. Every point of photoinduced spectra in Figs. 4–8 is the result of 100 laser shots. The measurements were carried out at room temperature in the air.

III. RESULTS

Figure 2 shows the electronic-absorption spectra, recorded for the same PANi film in EB and ES forms on a Shimadzu spectrometer. For EB, a sharp peak at $\lambda_{max}\cong 620$ nm ($\simeq 2.01$ eV) is observed. The spectrum of the salt form shows the sharp peak at $\lambda\simeq 360$ nm and an absorption band with a broad plateau from 760 to 1300 nm. The optical density D of ES decreases with a very gentle dip from the plateau to the boundary of the spectral region (2500 nm) diminishing three times. After heating to 68 °C, the general features of ES absorption spectrum are retained but a relatively small and broad maximum appears at 860 nm ($\simeq 1.45$ eV). With thermal heating from room temperature to 90 °C the low-energy absorption of EB shows a slight blueshift (the maximum shifts by 22 nm).

Figure 3 shows the difference thermal spectra, each spectrum being a difference of two absorption spectra recorded at elevated and room temperature. With increasing temperature the absorption spectrum for EB [Fig. 3(a)] varies the most essentially in the range of 650–800 nm. Here, heating leads to bleaching, which increases with temperature. Nevertheless, it can be seen from Fig. 3(a) that the D values at 370, 425, and 553 nm

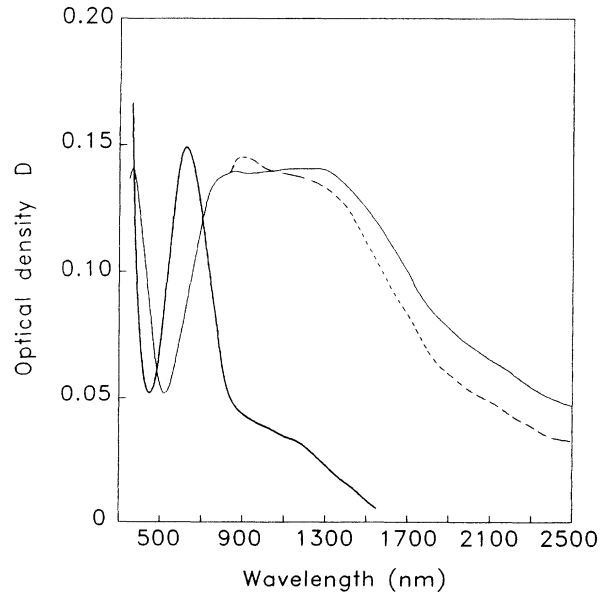

FIG. 2. Optical-absorption spectra of polyaniline film ($d=0.1$ μ) in various states: emeraldine base form (solid line, $t=25$ °C) and emeraldine salt form (line, $t=25$ °C and dashed line, $t=68$ °C).

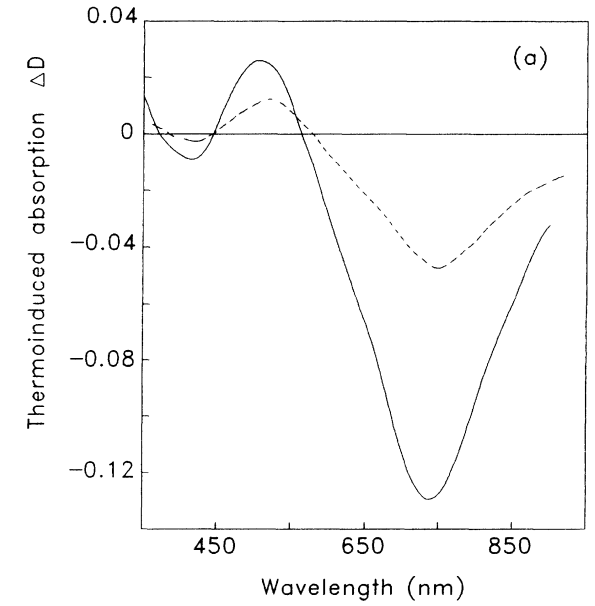

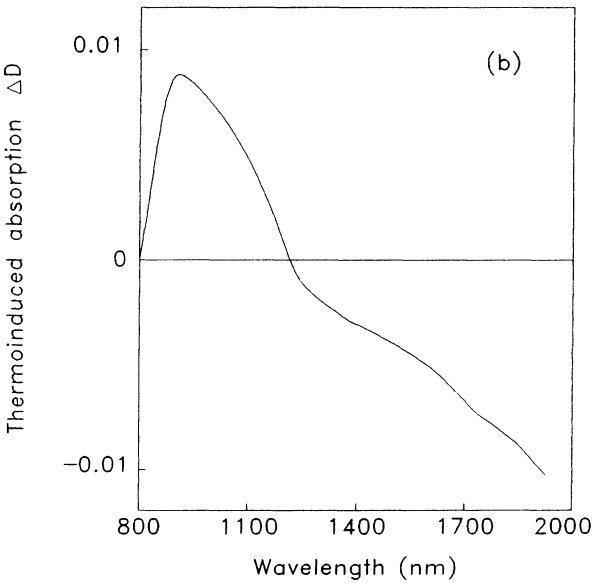

FIG. 3. Difference thermal-absorption spectra of polyaniline film ($d=0.2$ μ) in various states: (a) emeraldine base form [dashed line, $\Delta D=D(60\,°C)-D(25\,°C)$ and line, $\Delta D=D(90\,°C)-D(25\,°C)$] and (b) emeraldine salt form, $\Delta D=D(68\,°C)-D(33\,°C)$.

do not change practically with temperature. For ES [Fig. 3(b)] the changes of D with temperature are considerably smaller than for EB, with absorption increasing in the range of 850–1200 nm (thermoinduced absorption) and decreasing for $\lambda > 1200$ nm (thermoinduced bleaching).

Figure 4 shows the spectra of the photoinduced absorption ΔD_{ph} of EB film in the range 440–900 nm, where ΔD_{ph} is the difference of the D values for photoexcited and unexcited film. The photoinduced-absorption spectra were recorded at 300 K with two energies (P) of an excitation pulse (1 and 5 mJ/cm^2) for two different delay times (τ) between the pump-and-probe pulses ($\tau=0$ and 500 ps). The spectra in Fig. 4 with bleaching ($\Delta D_{ph} < 0$) in the region 550–800 nm with a maximum at 700 nm are similar. Beyond this region the ΔD_{ph} values are small or actually change sign to positive. The maxima of photoinduced-absorption spectra for $\tau=500$ ps show a slight redshift, of about 30 nm, in comparison to spectra for $\tau=0$.

Figure 5 shows the curves of photoinduced bleaching ΔD_{ph} at 555 and 660 nm for EB as a function of excitation pulse energy without pump-probe delay ($\tau=0$) and after a delay of $\tau=300$ and 600 ps, respectively. Figure 5(a) shows the monotonous dependence of ΔD_{ph} on P for the 555-nm bleaching without delay ($\tau=0$), where the bleaching change rate gradually diminishes with P growing. For bleaching with delay, the dependence is different: the ΔD_{ph} change rate at small P is lower than that in the case of $\tau=0$ and gradually grows. In the region of $P > 7.5$ mJ/cm^2 the values of ΔD_{ph} after a delay of $\tau=300$ ps become greater than those without delay. For the 660-nm bleaching [Fig. 5(b)] the general ΔD_{ph}-P relationship without delay and after a delay of $\tau=600$ ps is approximately the same as in the case of $\lambda_{probe}=555$ nm [Fig. 5(a)]. A linear dependence $\Delta D_{ph}(P)$ was observed for $\tau=600$ ps [Fig. 5(b)].

Figures 6–8 show dynamics of the changes of ΔD_{ph} for EB at $\lambda_{probe}=555$, 660, and 1066 nm for different energies of excitation pulse. In the bleaching band (Figs. 6 and 7) at a relatively low pulse intensity (2 mJ/cm^2) after an initial rapid growth of bleaching, a gradual decrease of bleaching with subsequent leveling off about 50–60 ps is observed. At a higher excitation intensity (10 mJ/cm^2) a monotonous transition of bleaching to a plateau near 50–80 ps is observed. In accordance with Fig. 4, the limiting value of $(-\Delta D_{ph})$ in Figs. 6 and 7 for $P=10$ mJ/cm^2 is greater than the one for 2 mJ/cm^2. The full relaxation of the absorption spectrum to the initial state

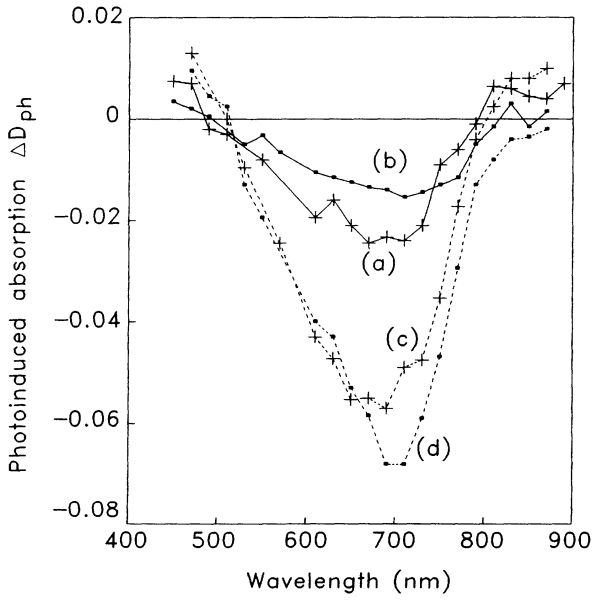

FIG. 4. Photoinduced absorption spectra of the emeraldine base film ($d=0.15$ μ) for different pulse intensity and pump-probe delay: (a) $P=1$ mJ/cm^2, $\tau=0$, (b) $P=1$ mJ/cm^2, $\tau=500$ ps, (c) $P=5$ mJ/cm^2, $\tau=0$, (d) $P=5$ mJ/cm^2, $\tau=500$ ps.

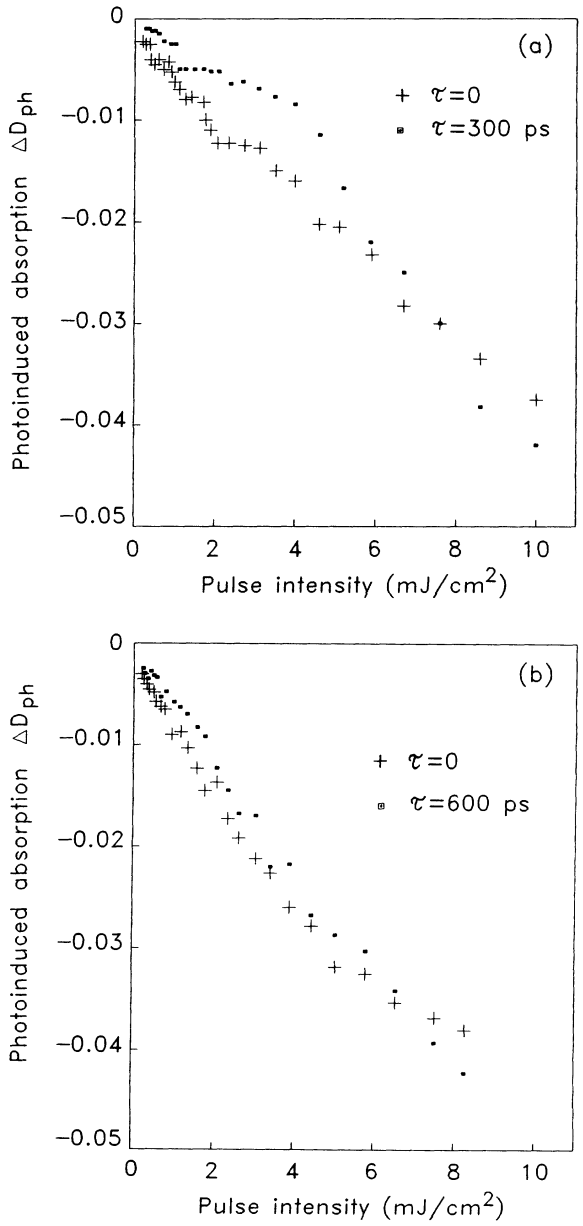

FIG. 5. Photoinduced bleaching at 555 nm (a) and 660 nm (b) for the emeraldine base film ($d=0.15$ μ) as a function of the pulse intensity for different pump-probe delay (τ).

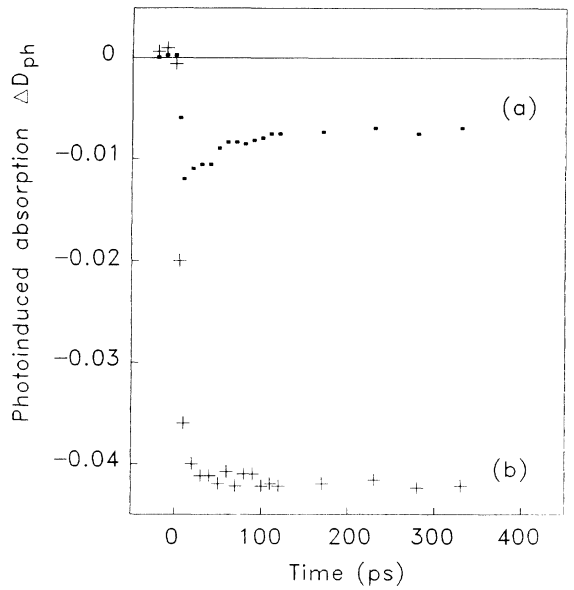

FIG. 6. Dynamics of the changes of the photoinduced bleaching at 555 nm for the emeraldine base film ($d=0.15\ \mu$) as a function of the pump-probe delay for two pulse intensities: (a) $P=2$ mJ/cm^2 and (b) $P=10$ mJ/cm^2.

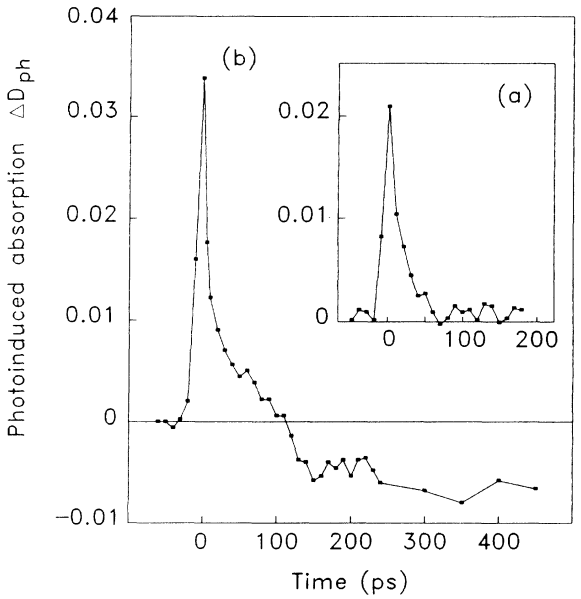

FIG. 8. Dynamics of the changes of the photoinduced absorption at 1066 nm for the emeraldine base film ($d=0.15\ \mu$) as a function of the pump-probe delay for two pulse intensities: (a) $P=1$ mJ/cm^2 and (b) $P=10$ mJ/cm^2.

(the absorption spectrum prior to laser attack) takes place for 5–10 min at room temperature. The rapidly growing part of the bleaching dependence in Figs. 6 and 7 was found to fit either a single exponential function $A\exp(-t/\tau_1)$ with characteristic time $\tau_1\simeq 170$ ps or a power law of the form $t^{-\delta}$ with $\delta\simeq 0.2$.

The photoinduced absorption at $\lambda_{\text{probe}}=1066$ nm (Fig. 8) for $P=1$ mJ/cm^2 vanishes in 100 ps with a characteristic time $\tau_1\simeq 17$ ps. At greater energy of excitation (10 mJ/cm^2) the photoinduced absorption decays to zero in 100 ps with characteristic time $\tau_1\simeq 30$ ps. Afterwards, photoinduced bleaching takes place, which practically does not change after 150 ps in the ps range.

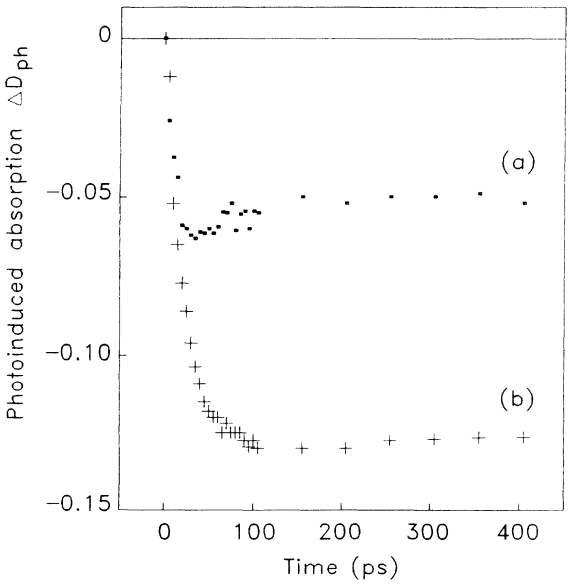

FIG. 7. Dynamics of the changes of the photoinduced bleaching at 660 nm for the emeraldine base film ($d=0.15\ \mu$) as a function of the pump-probe delay for two pulse intensities: (a) $P=2$ mJ/cm^2 and (b) $P=10$ mJ/cm^2.

IV. DISCUSSION

A. Absorption spectra and electronic structure of conjugated fragments of polyaniline

The electronic-absorption spectra of the EB and ES films at 25 °C (see Fig. 2) are very similar to those observed by Monkman and Adams[10] for the films synthesized chemically and with by-products carefully eliminated. The optical density D in the near-IR range for ES (Fig. 2) decreases rather quickly as the wavelength increases in comparison with the Monkman-Adams[10] case. These differences are probably due to different conditions of film preparation. As noted by many authors,[28–30] different methods and conditions of synthesis and protonation (deprotonation) of the films affect the electronic spectra of the EB and ES films. We also noted poor reproducibility of ES spectra in the low-energy range even though identical synthesis conditions were used for all samples.[28] The change of the ES spectrum, upon slight heating [the appearance of the maximum at 860 nm ($\simeq 1.4$ eV) (see Fig. 2)], points to a complex structure of the low-energy absorption. According to Monkman *et al.*,[28] the first maximum in the ES spectrum corresponds exactly to 1.4 eV.

The optical density D of EB decreases steeply in the region from $\lambda_{\max}\cong 620$ nm ($\simeq 2$ eV) to $\lambda_1\cong 800$ nm ($\simeq 1.55$ eV) and much more gently from λ_1 to $\lambda_0\cong 1600$ nm

($\simeq 0.8$ eV). A similar picture is observed for the low-energy absorption of other polymers with conjugated bonds. For example, the energies corresponding to λ_{max}, λ_1, and λ_0 in the spectra of polyacetylene[31] and poly-(*p*-phenylenevinylene) (Ref. 32) have the following values: 1.9 and 2.5 eV (λ_{max}), 1.3 and 2.35 eV (λ_1), and 0.8 and 2 eV (λ_0), respectively. It is worth noting that in the case of very carefully prepared EB films (see Ref. 10) the region with slow decreasing absorption is absent: $\lambda_0 \cong \lambda_1 \cong 850$ nm (1.47 eV) and $\lambda_{max} \cong 610$ nm (2.03 eV).

We believe that the first maximum in the low-energy absorption is due to the electron transitions among delocalized π electron molecular orbitals (MO). The arguments supporting this point of view are presented below.

Consider the electronic structure of a long polymer chain of PANi obtained by means of the valence effective Hamiltonian technique.[33,34] The calculation predicts the band gap E_g for the LB form of about 4.4 eV consistent with the transparency of this material to the eye.[33] We may also note that according to the calculation,[34] the first interband transitions in the EB and ES chains appear between π bands and have the energies $\Delta E_{\pi\pi^*} \leq 1.5$ eV. Consequently, the energy ΔE_1 of the first maximum in the absorption spectrum of a long CF is determined by the electron transitions between delocalized states of this CF. However, the correct value of ΔE_1 can be obtained only when the effects of electronic correlations are taken into consideration. This is accomplished by performing the configuration interaction (CI) calculations for both the ground and the excited state of CF's (see, for example, Ref. 35). Sjögren and Stafström[36] investigated the electronic excitations in aniline tetramers using the INDO/*S*-CI method. In the CI, 300 singly and doubly excited lowest-energy configurations were chosen from the 5000 generated. The value of ΔE_1 was found to be 3.6, 2.3, and 1.5 eV for tetra-aniline oligomers of LB, EB, and ES types, respectively,[36] in accord with experiment.[37]

These calculations show the great importance of the electron-electron interactions and display the proximity in ΔE_1 values for polyaniline systems of different types (EB, ES, and PNB). The following reasoning comments and explains this proximity. The dominant importance of the electron-electron interactions makes it possible, in the first approximation, to ignore differences in bond lengths, chain charges, and in the number of hydrogen atoms in the σ core for the PANi structures in Fig. 1. Then all the PANi structures (in this approximation) consist of the same aniline fragments and are distinguished only by the number of π electrons. Each aniline fragment (or lattice cell) has seven atomic orbitals yielding seven MO's. Two of these MO's are localized on the phenyl ring and exert no influence on the low-energy excitations. One of these local MO's is always occupied by the two π electrons and the other one is always empty. Each aniline fragment contributes five MO's to the chain conjugation system; they form five electron energy bands, which can be occupied by the delocalized π electrons. Now let us estimate the number of electrons on one fragment and thus determine the electron occupancy of the energy bands. For LB, each aniline cell contributes six π electrons ($8-2$ localized), three bands are completely occupied, and the electron excitations, which are caused by *interband* electron transfers, are characterized by a large ΔE_1 value ($\cong 3.5$ eV). For EB and ES we have 5.5 electrons in each cell, and for PNB we have 5 electrons per cell. For all these structures (from the viewpoint of band theory) the upper band of the chain is partially occupied. For this reason EB, ES, and PNB can be combined into one group where the electron excitations, which are caused by *intraband* electron transfers, are characterized by a relatively low ΔE_1 value (from 1.4 eV for ES and PNB to about 2 eV for EB).

As the chain length increases, the value of ΔE_1^{exp} decreases from $\simeq 2.4$ eV for the imine trimer to $\simeq 2.1$ eV for the polyemeraldine base (EB).[38] Such behavior of ΔE_1^{exp} reveals that the first maximum in the absorption spectra is related to π MO's delocalized over a whole CF. Such a decrease of ΔE_1^{exp} to a limiting value is a characteristic property of long CF's.[35] The ΔE_1^{exp} values of the imine trimer and the tetramer of EB type are very close to those of EB polymers. However, we believe that this fact does not imply that the 2-eV absorption is due to the creation of a molecular exciton associated with a locally distorted segment of the "polyaniline" backbone, as suggested by Duke, Conwell, and Paton.[39] Inasmuch as the trimer and the tetramer of aniline are already rather long CF's involving, respectively, $n = 13$ and 19 effective conjugated bonds along the backbone (a phenyl ring includes three effective bonds in the backbone), the change in the ΔE_1 values with subsequent lengthening of an oligomer backbone should not be large. It should be pointed out that polyenes with such a length also have ΔE_1^{exp} very close to the limiting value $\Delta E_1^{exp}(\min) \simeq 2.2$ eV observed for very long polyenes: $[\Delta E_1^{exp} - \Delta E_1^{exp}(\min)] \simeq 0.5$ eV for the 18-annulene with $n = 18$.[35,40]

The phenyl rings of PANi chains are often believed to be twisted out of the plane formed by the nitrogens by a large angle $\phi \geq 50°$. Such large tilt angles interrupting the conjugation along a chain backbone were obtained in modified neglect of differential overlap calculations for the ground states of aniline trimers [of LB and PNB types, Figs. 1(a) and 1(b)] and in complete neglect of differential overlap (CNDO/*S*3) calculations for electronic excitations of such molecules.[41] However, experimental oligomer data have indicated angles of about $\pm 15°$ for the polymer in the ES form.[42] On the other hand, according to the study of the crystallinity of the various forms of PANi together with the parameters of their structure presented by Pouget *et al.*,[18] the twist angles ϕ of phenyl rings, $\phi \cong 30°$ for EB and $\phi \cong 0$ for ES, are obtained. Hence, these angles are considerably smaller than it was previously assumed. Therefore, the conjugation in the PANi backbone does not seem to be interrupted by such tilt angles because the π electron parameters of interatomic hopping for C-N bonds are diminished by not more than $(1-\cos\phi) \cong 14\%$ due to this twisting. This conclusion is supported by the calculations of the absorption spectra of the EB form of aniline tetramers: the first maximum at 2 eV is retained for $\phi \leq 40°$ and disappears for larger angles ($\phi \geq 60°$).[36,39] Calculations of absorption and luminescence spectra for short oligomers[36,38,41] gave tilt angles of $\phi \leq 20°-30°$ for the best correspondence

with experiment. Observing only a minor contribution of the Raman-active modes to the IR spectrum of EB, Kim *et al.*[9] also concluded that the average conjugation length of a polymer chain in their sample is large enough.

Large phenyl-ring rotations with $\phi > 40°$ are unlikely to take place in PANi at room temperature, because high energy is required for the breakdown of conjugation in a chain ($\simeq 1$ eV for one π bond) due to an increase in the π electron energy. Large ring rotations may occur only in the course of synthesis or doping reactions. They play the role of chain defects dividing the polymer chains into CF's. The addition of hydrogen to a chain backbone may also be responsible for defect generation on a chain. In the case of polyacetylene the methylene group —CH_2— is a dominant chain defect breaking conjugation in a chain.[43,44] The concentration of these breaking defects is inversely proportional to the average conjugation length or the average length of CF's.

All parts of a CF backbone with small tilt angles ($\phi \leq 30°$) are conjugated equally well because the parameter β for π electron hopping is approximately the same for all chain bonds. In this case, both the charge which gets on a CF and the electron, which hops from one π MO to another during absorption of light, delocalize over a whole CF. Calculations of the electronic structure of ions of long polyenes and other conjugated hydrocarbons show that the electronic charge is delocalized over a whole molecular ion (see, for example, Ref. 45). We think that the positive charge on an ES chain with $\phi \cong 0$ is also delocalized over all atoms of a chain rather than located only on the nitrogens as it is usually represented on the molecular structures [see Fig. 1(c)]. In fact, in the case of the ES tetramer it was observed that the positive charges are delocalized over all the nitrogens and all the rings.[42] Therefore, for PANi with small ϕ, there is no reason to introduce the defect states with rotation of each ring and with electron transfer from one phenyl ring to another, as suggested by McCall *et al.*[5]

We believe that delocalization of π MO's over the whole CF is the most important property of conducting polymers that differ from usual molecular crystals only in the size of the molecules, the word "molecule" being taken to also include a CF.

The average length of CF's in PANi can be estimated as the crystalline domain size L deduced from an x-ray study of PANi by Pouget *et al.*[18] For EB samples L ranges from 30 to 100 Å (EB-I type of structure) or from 50 to 150 Å (EB-II type). For ES samples L ranges from 20 to 55 Å.[18] Considering the tetramer length $t \cong 20$ Å as a natural unit of chain length, we conclude that L ranges from $3t$ to $7t$ for EB and from t to $3t$ for ES.

B. A model of charge-transfer excitons

As it has been explained above, the first maximum in the low-energy absorption of EB and ES appears due to π-π^* electron transitions in the separate CF's. We suppose that the charge-transfer excitons (CTE's) appear in the polymer material upon photoexcitation. The charge carriers (electrons) are delocalized over several CF's surrounding the excited CF. We propose that the geometry and the electronic structure of CTE's determine the shape of the low-absorption band and other properties of the photoexcited PANi. Since all the CF's are not equivalent, the excitation cannot propagate through the polymer sample because of the lack of translational symmetry. Thus, we consider only a localized exciton associated with excited CF's. The second argument against any mobility of excitations is the invalidity of the band model for the systems composed of the molecules bound by weak interactions (molecular crystals). The zeroth-order wave function for such systems is the product of functions of isolated molecules rather than the product of the Bloch states of the band theory. This question was treated in more detail in concern with the cooperative effects in quasi-one-dimensional crystals.[46]

The states of a localized CTE involve the excited state of one CF and the states where one of its electrons is transferred from its highest-occupied MO (HOMO) to the lowest-unoccupied MO (LUMO) of a neighbor CF. These states appear when one photon with energy $\hbar\omega \simeq \Delta E_1 \simeq 2$ eV is absorbed. To make such a transfer possible, the following energy relation has to be satisfied:

$$I - A - 2E_d \simeq \Delta E_1 , \tag{1}$$

where I is the ionization potential of the CF, A is the electron affinity of the CF, and E_d is the polarization energy or the energy of the electronic polarization of the neutral CF's placed in the Coulomb field of the charged CF's with an excessive or deficient electron. Analyzing the available data on I, A, and E_d for the large molecules with conjugated bonds, one can find that in polyacetylene $I \simeq 6.6$ eV, $A \simeq 1$ eV, and $E_d \simeq 1.5$–1.9 eV.[20,45,47,48] In a similar way, we suppose that these parameters in the case of EB can be estimated as follows: $I \simeq 6$ eV, $A \simeq 1$ eV, and $E_d \simeq 1.5$ eV. Then one obtains about 2 eV on the left-hand side of Eq. (1), i.e., requirement (1) is fulfilled because $\Delta E_1 \simeq 2$ eV in the case of EB. The left-hand side of Eq. (1) is just the energy required for generation of two separated charges located on the CF's i and j denoted below as CF_i^+ and CF_j^-. A more detailed energy condition for appearance of such charged fragments is as follows:

$$I - A - G_{ij} - E_{\text{pol}} \simeq \Delta E_1 , \tag{2}$$

where $(-G_{ij})$ is the Coulomb interaction energy of the two charged CF's and E_{pol} is the polarization energy which involves the contributions $E_{\text{pol}}^{\text{CF}}$ from polarization of all the other CF's in the Coulomb field of two charged fragments and two contributions, $E_{\text{pol}}^{(+,i)}$ and $E_{\text{pol}}^{(-,j)}$, from the mutual polarization of CF_i^+ and by CF_j^- and vice versa:

$$E_{\text{pol}} = E_{\text{pol}}^{\text{CF}} + E_{\text{pol}}^{(+,i)} + E_{\text{pol}}^{(-,j)} . \tag{3}$$

Born,[49] Klemm,[50] and Overhauser[51] considered the excited states of alkali-halide crystals arising from the electronic configuration with an electron transferred from a negative halide ion to a nearest alkaline positive ion. In this case the exciton state in the crystal was considered as that involving the electronic configurations with electrons transferred between the lattice atoms only. In the

case of conducting polymers, the electron transfer merely accompanies the electronic excitation of a single CF. It should be noted, however, that electron transfer will be important for the excitations of higher energy if the condition Eq. (1) is not satisfied, for example, when

$$I - A - G_{ij} - E_{\text{pol}} \gg \Delta E_1 \ .$$

As the motion of electrons in a conducting polymer takes place in an irregular lattice composed of nonequivalent CF's, the hopping parameters are different and the momentum of the electron is not an integral of motion and thus it is a bad quantum number. For this reason, any electronic perturbation associated with any group of CF's is local and conserves its locality. The main interactions to be considered in the CTE problem are the Coulomb interaction of two ions, CF_i^+ and CF_j^-, the electronic polarization of the surrounding medium induced by these ions, and the resonance interaction (electron hopping) of neighboring CF's. The hopping parameters t_{kl} for the electron transfer between the HOMO's or LUMO's of neighboring chains are significant (about 0.1 eV due to the dense packing of the polymer chains). For polyacetylene, where packing of the chains is very dense, the maximal value of t_{kl} was estimated ca. 0.3 eV.[20] Looser packing of the respective chains of other conducting polymers results in the substantial decrease in t_{kl} values as compared to polyacetylene.

Let us assume that the EB and ES chains are packed as in the EB-II and ES-I structures,[18] respectively. These structures correspond to the PANi samples obtained electrochemically as in this work. We construct a model of CTE consisting of one CF, a, which absorbs one photon, and N CF's which surround the CF a. For the sake of simplicity, we assume that all the CF's are of the same length L, equal to the average conjugation length of EB or ES. In Figs. 9 and 10, a simple symmetrical model CTE is shown. It contains the shell of $N=34$ CF's. Eight CF's form the first layer of the CTE shell, and the resting 26 CF's form the second layer. The neighbor CF's in CTE are all shifted by one-half of the CF length with respect to each other. Their relative orientations are also the same. For this reason, all the hopping parameters t_{kl} are the same, $t_{kl}=t_0$, and are equal to one-half the value of the parameter t for the CF's with no relative translation of the two neighboring fragments. To take into account the actual disorder that occurs in PANi, we must treat the situation with different $t_{kl}\neq t_0$, as it was done in Ref. 20.

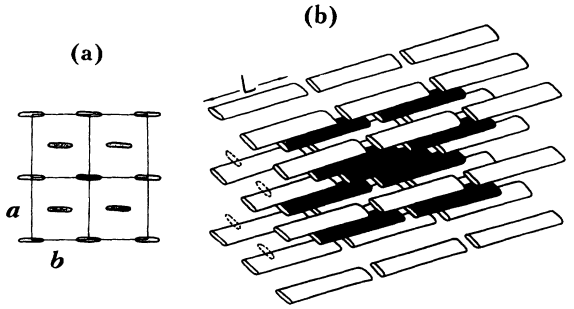

FIG. 9. Model of the charge-transfer exciton (CTE) in emeraldine base: (a) projection along the axis of conjugated fragments (CF's) and (b) side view on the CTE with a central fragment α (black), 8 CF's of the first layer of the CTE shell (grey) and 26 CF's of the second layer. $a=7.65$ Å, $b=5.75$ Å, as for the EB-II structure from Ref. 18.

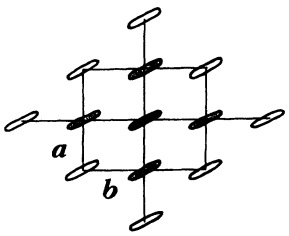

FIG. 10. Model of the charge-transfer exciton in emeraldine salt: projection along the axis of conjugated fragments. Side view is the same as in Fig. 9(b). $a=4.3$ Å, $b=5.9$ Å, as for the ES-I structure from Ref. 18.

Let the CF a, which absorbs a photon and undergoes the permitted transition from the ground state $\psi(a)$ to some excited state $\psi^*(a)$, be surrounded by the fragments $b_1, b_2, b_3, \ldots, b_N$. The variational wave function of this exciton, ψ(CTE), can be taken in the simple hydrogen-atom form:

$$\psi(\text{CTE}) = c_0\psi_0^*(a) + c_1\psi_1 + c_2\psi_2 + c_3\psi_3 + \cdots c_N\psi_N \ . \tag{4}$$

Here c_0 and c_i are the variation coefficients and the basis functions ψ_i are given by

$$\psi_i \equiv \psi(a^+ b_1 b_2 \cdots b_{i-1} b_i^- b_{i+1} \cdots b_N) \ .$$

They are the many-electron wave functions for the $N+1$ fragments, where an electron taken from a is placed on b_i, and the other neutral b_j CF's ($j\neq i$) are polarized. We take this basis function approximately as the product of the wave functions of the separate unpolarized fragments

$$\psi_i \cong \psi_0(a^+)\chi(b_1)\chi(b_2)\cdots\chi(b_{i-1}) \times \chi(b_i^-)\chi(b_{i+1})\cdots\chi(b_N) \ .$$

To simplify the description we assume that (i) electronic excitation of the fragment a is the transfer of an electron from the HOMO of a (the electron annihilation operator is a_σ) to the LUMO of a (the electron creation operator is A_σ^+), (ii) ionization of a can be presented as removing an electron from the HOMO of a (the electron annihilation operator is a_σ), and (iii) formation of the anion b_i^- can be described as creation of an electron in the LUMO of the fragment b_i (the electron creation operator is $B_{i\sigma}^+$).

Then for the singlet excited states the basis functions can be written as

$$\begin{aligned} &\psi_0(a) = a_\alpha^+ a_\beta^+ |0\rangle_0 \ , \\ &\psi_0^*(a) = 2^{-1/2}(A_\alpha^+ a_\beta^+ - A_\beta^+ a_\alpha^+)|0\rangle_0 \ , \\ &\psi_i = 2^{-1/2}(B_{i\alpha}^+ a_\beta^+ - B_{i\beta}^+ a_\alpha^+)|0\rangle_0 \ , \end{aligned} \tag{5}$$

where

$$|0\rangle_0=\psi(a^{++})\chi(b_1)\chi(b_2)\cdots\chi(b_N)$$

is the product of the N wave functions of the fragments b_k in their ground states, $\chi(b_k)$, and the wave function $\psi(a^{++})$ for the fragment a with two electrons removed from the HOMO.

It is known[50] that the energy of the electronic polarization of all the atoms of a crystal with the NaCl lattice and two charges ($+e$ and $-e$) located at the two neighboring atoms of the crystal four times exceeds the energy of the mutual polarization of the two neighboring atoms themselves. We assume that the same ratio holds for our model crystal composed of the similar CF's (see Figs. 9 and 10). Thus, if the fragments i and j are the neighbors, we have

$$E_{\rm pol}^{\rm CF}/(E_{\rm pol}^{(+,i)}+E_{\rm pol}^{(-,j)})\simeq 4$$

and from Eq. (3) we obtain

$$E_{\rm pol}\cong 5(E_{\rm pol}^{(+,i)}+E_{\rm pol}^{(-,j)})\ . \tag{6}$$

In polyacetylene (PA) the energy of the mutual polarization of the two long ($l\simeq 40$–60 Å) charged-neighbor CF's has been estimated in Refs. 20 and 52 as

$$E_{\rm pol}^{(+)}({\rm PA})=E_{\rm pol}^{(-)}({\rm PA})\cong 0.25\text{–}0.30\ {\rm eV}\ . \tag{7}$$

Considering Eqs. (3), (6), and (7), and the similarity of π electronic structure of CF's and their mutual arrangements in PANi and PA, we assume that

$$E_{\rm pol}^{(+,i)}=E_{\rm pol}^{(-,j)}=E_{\rm pol}^{(+)}({\rm PA})=E_{\rm pol}^{(-)}({\rm PA})$$

and as a result the total polarization energy in polyaniline resulting from the two-neighbor-charged CF's is estimated, according to Eqs. (6) and (7), as follows:

$$E_{\rm pol}\cong 5(E_{\rm pol}^{(+,i)}+E_{\rm pol}^{(-,j)})\cong 2.5\text{–}3.0\ {\rm eV}\ . \tag{8}$$

This rough estimate shows that the total polarization energy from the close ($E_{\rm pol}\simeq 2.5$–3 eV) and the distant ($2E_d\simeq 3$ eV, see above) charged CF's is approximately the same: $E_{\rm pol}\cong 2E_d$. This consideration enables us, in the zeroth approximation, to avoid the necessity of estimating $E_{\rm pol}$ for other mutual displacements of the charged pairs of CF's in the exciton shell and to take the energy

$$E_0=I-A-2E_d=I-A-E_{\rm pol} \tag{9}$$

as the zero energy.

The coefficients c_n^k in the expansion, Eq. (4), for the function ψ(CTE) and the energies E_k of all the exciton states are determined after solving the secular equation constructed with the basis functions ψ_0, ψ_i, and $i=1,\ldots,34$, Eq. (5). Off-diagonal elements of the secular matrix are the matrix elements of the resonance operator $H_{\rm res}$ for each pair of the basis functions ψ_0 and ψ_i. The resonance operator, describing the transfers of electrons between fragments, has the form:

$$H_{\rm res}=\sum_{i\sigma}t_{0i}(a_\sigma^+B_{i\sigma}+B_{i\sigma}^+a_\sigma)+\sum_{ij\sigma}t_{ij}(B_{i\sigma}^+B_{j\sigma}+B_{j\sigma}^+B_{i\sigma})\ ,$$

where the first term describes the electron hopping between the central fragment a and its nearest neighbors in the first layer and the second term describes the electron hopping between the other nearest fragments in the exciton shell. The diagonal element of our secular matrix corresponding to the basis function ψ_i will be equal to $(-G_i)$, where $(-G_i)\equiv(-G_{ai})<0$ is the Coulomb interaction energy of the central cation a^+ and the ith anion. The energies $(-G_i)$ will be estimated in a model of the uniformly charged thin rods of the length L which substitute the charged CF's. The diagonal matrix element corresponding to the basis function $\psi_0^*(a)$, is equal to ΔE_1-E_0, as all of the diagonal matrix elements are shifted down by E_0. The next section contains some qualitative results of calculations of exciton absorption in polyacetylene and polyaniline.[52]

C. Structure of low-energy absorption band

Considering the matrix of the Hamiltonian for the charge-transfer exciton in EB, we can note that the difference between the diagonal energies $(-G_i)$ and $(-G_j)$ of the Coulomb interaction of the neighbor anions i and j with the central cation a^+ (Fig. 9) surpasses $\simeq 0.3$ eV, and the inequality

$$\delta G_{ij}\equiv|G_i-G_j|\geq t_{ij}$$

holds. This inequality ensures the localization of the transferred electron in a relatively small volume on a few dozens of CF's, surrounding the central fragment a (the nearest and the next-nearest neighbors of a, which form the first and the second layers of the exciton shell) and even (with the reasonable accuracy) in the first layer of the exciton shell (the nearest neighbors of a). In ES composed of the long multicharged CF's, the energy of their interactions is proportional to the product of their charges. However, at the electron transfer between the equally charged CF's in ES, the Coulomb repulsive energy keeps decreasing by the energy of interaction G_{ij} of the two single-charged ions, as in EB. It is precisely this change of energy of the system at the charge transfer which is to be considered as the energy of the basis state ψ_i [Eq. (4)] corresponding to the charge transfer in our exciton model having the similar CF's.

We estimate the maximum ($G_{\rm max}$) value of G_i for the first layer of the exciton shell and the minimum ($G_{\rm min}$) value for the second one. It turns out that $G_{\rm max}=1.05$ eV and $G_{\rm min}=0.4$ eV for ES with $L=40$ Å and $G_{\rm max}=0.8$ eV and $G_{\rm min}=0.25$ eV for EB with $L=70$ Å. For anions in the outer layer which correspond to the Onsager radius, a rough estimate $G_{\rm min}\simeq kT$ seems to hold. That is why the width of the exciton band $\simeq(G_{\rm max}-G_{\rm min})\simeq G_{\rm max}$ is about 1 eV. The parameters of the electron hopping $t_{ij}\simeq 0.1$ eV are much smaller than the $G_{\rm max}\simeq 1$ eV and thus do not affect the exciton bandwidth.

Let us consider the lower limit $\Delta E_{\rm min}$ of the exciton absorption and the position of this limit with respect to the absorption maximum. In the case of EB we obtain the following estimate:

$$\Delta E_{\min}(\mathrm{EB}) = I(\mathrm{EB}) - A(\mathrm{EB}) - 2E_d(\mathrm{EB}) - G_{\max}(\mathrm{EB})$$
$$\simeq \Delta E_1 - G_{\max}(\mathrm{EB}) \simeq 1.2 \text{ eV} \quad (10)$$

in accord with the experimental data (see, for an example, Fig. 2).

The intensity of the exciton absorption band first of all depends on the intensity of the electron transition in the CF a. Actually, the matrix element of the operator of the dipole length $\hat{R}$ for the transition from the ground state $\psi(a)$ of the CF a to the kth state of the exciton band

$$\psi_k(\mathrm{CTE}) = c_{0k}\psi^*(a) + c_{1k}\psi_1 + c_{2k}\psi_2 + \cdots + c_{Nk}\psi_N ,$$

with the energy E_k reads

$$\langle \psi(a)|\hat{R}|\psi_k(\mathrm{CTE})\rangle = \langle \psi(a)|\hat{R}|\psi^*(a)\rangle c_{0k} . \quad (11)$$

The intensity of the electronic transition to the kth state, I_{0k}, is proportional to the square of this matrix element,

$$I_{0k} \simeq |\langle \psi(a)|\hat{R}|\psi^*(a)\rangle|^2 {c_{0k}}^2$$

and the normalization condition for c_{0k} is

$$\sum_{\text{all } k} {c_{0k}}^2 = 1 .$$

Therefore, the intensity of the transition $\psi(a) \Longrightarrow \psi^*(a)$ in the isolated CF is now distributed over the entire exciton band. The intensity of the absorption maximum in the sample decreases as compared to that of the isolated fragment. In the vicinity of the absorption maximum, there are several intensive transitions to the states with the close energies $E_k \simeq \Delta E_1$. When the energies of the excitations to the states $\psi_k(\mathrm{CTE})$ are different enough from the energy at the absorption maximum, the intensities of the corresponding transitions become small[52] due to the small values of ${c_{0k}}^2$.

Values of t_{ij}, determining the intensity of the low-energy band, depend on the structure and packing of CF's and evidently decrease in the polyacetylene, polyaniline, and polyphenylenevinylene series. Within the framework of our model this decrease is naturally in agreement with the fact that for polyacetylene the low-energy band does not practically segregate from the main maximum,[31] whereas for polyphenylenevinylene the low-energy band is detached in the independent band of the spectrum in the region from λ_1 to λ_0 and it can be distinguished by its low intensity.[32]

The position of the low-energy maximum in the ES absorption spectrum is determined by the absorption spectrum of the long charged polyaniline CF's. The spectrum of the cation T^{2+} of the aniline tetramer T of LB, has the maximum at $\Delta E_1^{\exp} \simeq 1.2$–$1.3$ eV.[37] For the PANi films in various degrees of oxidation (close to ES) it was found that $\Delta E_1^{\exp} \simeq 0.7$–$1.4$ eV (Ref. 28) and $\Delta E_1^{\exp} \simeq 1.5$ eV.[30] As it will be shown below, a remarkable feature of ES is that the lower limit $\Delta E_{\min}$ of the exciton absorption is approximately zero.

The energy of the lower limit of the exciton absorption in ES is expressed as

$$\Delta E_{\min}(\mathrm{ES}) = I(\mathrm{ES}) - A(\mathrm{ES}) - 2E_d(\mathrm{ES}) - G_{\max}(\mathrm{ES}) . \quad (12)$$

Let us suppose that ES consists of the charged fragments ${T_2}^{4+}$ with the length $L = 40$ Å, where T is the aniline tetramer of the LB type. The electron affinity of ${T_2}^{4+}$ is the fourth ionization potential of the neutral fragment T_2, $A(\mathrm{ES}) = I_4(T_2)$, and the ionization potential of ${T_2}^{4+}$ is the fifth ionization potential of T_2, $I(\mathrm{ES}) = I_5(T_2)$. Expression (12) includes the difference of the two successive ionization potentials. To estimate these potentials we can consider the well-known example of linear polyenes. When the long polyene chains have been calculated in the π electron approximation with account of the Coulomb interaction of π electrons, it was found[45] that (i) successive potentials of ionization $I_1 \equiv I$, I_2, and I_3 for long polyenes (with number of carbon atoms $N > 20$) change slightly with the growth of N (decrease within 5%) and (ii) for the long polyenes

$$I_2 = I_1 + \delta_1 \quad \text{and} \quad I_3 = I_2 + \delta_2 , \quad (13)$$

where $\delta_1 = 1.3$ eV and $\delta_2 = 1.5$ eV.

For the long CF's of polyaniline the difference $\delta = (I_{n+1} - I_n)$ may be estimated as $\delta \cong 1.5$ eV, as for the lowest three ionization potentials of the long polyenes. On the other hand, on the basis of the Koopmans theorem[53] (in self-consistent field approximation) we obtain an estimate for δ in the form of the difference of the successive energies ε_n of molecular orbitals:

$$\delta = (I_{n+1} - I_n) \simeq \varepsilon_n - \varepsilon_{n+1} . \quad (14)$$

This suggests that $\delta \simeq 1$ eV for the long polyene molecule, because the difference of the successive energies ε_n decreases with the increase of the molecule length. Thus, estimates for δ in a variety of ways give the same value for δ, namely $\delta \simeq 1.5$ eV. The electronic polarizability of the ES fragments in the considered processes is strongly diminished as compared to the polarizability of the EB fragments since the ES fragments were quite polarized particularly by the point charges (Cl^-), and thus $E_d(\mathrm{EB}) \gg E_d(\mathrm{ES}) \simeq 0.1$ eV. As $G_{\max}(\mathrm{ES}, L = 40$ Å$) \cong 1.1$ eV, we obtain

$$\Delta E_{\min}(\mathrm{ES}) = I(\mathrm{ES}) - A(\mathrm{ES}) - 2E_d(\mathrm{ES}) - G_{\max}(\mathrm{ES})$$
$$\cong \delta - G_{\max}(\mathrm{ES}) - 2E_d(\mathrm{ES}) \simeq 0 . \quad (15)$$

This estimate $[\Delta E_{\min}(\mathrm{EB}) \gg \Delta E_{\min}(\mathrm{ES}) \simeq 0]$ is in agreement with the observation that the low-energy band in the ES absorption spectrum is extended to the near-IR region and also with the fact that ES has the metal-like conductivity.[54,55] Actually, the right-hand side of Eq. (15) is nothing but the minimal energy required for the electron transfer from one CF to another. As this energy is very small, approximately no energy is spent on the electron transfer, which is the main characteristic feature of a metallic state.

D. Thermostimulated and photoinduced spectra

The blueshift of the absorption bands of EB and ES films observed at higher temperature is a common feature of UV spectra of polyatomic molecules in the condensed phase. It is usually attributed to the change of the dielec-

tric constant of the medium in the framework of, say, the Onsager model.[56–59] The blueshift of the broad maximum in the absorption spectrum results in the bleaching maximum (in the region of the long-wavelength slope of the broad absorption maximum) and in the additional absorption maximum (in the region of short-wave slope of the broad absorption maximum) in the difference thermostimulated spectrum. That is precisely what is shown in Fig. 3 where the maxima are the differences of the two broadbands and cannot be assigned to specific states of the polymer chains.

The difference spectrum of EB, measured at temperatures ranging from 300 to 390 K [Fig. 3(a)], slightly differs from the spectrum obtained by Roe *et al.*[8] for temperatures ranging from 15 to 300 K. Ginder *et al.*[60] also observed the blueshift of the absorption maximum when the EB film was heated over room temperature. Their value of the shift ($\simeq 1$ meV/K) coincides with our data. Thus, the thermal heating of the EB film over the room temperature results in the appreciable changes of the spectrum particularly in the long-wavelength region. The heating up to 60 °C reduces the maximum of the optical density to $\simeq 0.05$ [Fig. 3(a)]. This value has the same order of magnitude as that obtained by the photoinduced bleaching with the energy of laser pulse 5 mJ/cm^2 (see Fig. 4). For this reason we take into account the photoinduced warming up of the sample when we interpret our experimental results on EB. The thermal heating does not change the optical density at 400, 426, and 553 nm [see Fig. 3(a)], so here the photoinduced phenomena are present in their pure form.

The photoinduced spectra of EB (Fig. 4) resemble each other and are also similar to the photoinduced spectrum obtained by Kim *et al.*[9] in the steady-state measurements, where the photoinduced bleaching with maxima at 680 nm (1.8 eV) and 338 nm (3.7 eV) and the photoinduced absorption with maxima at 1400 nm (0.9 eV), 900 nm (1.4 eV), and 417 nm (3 eV) were observed. Besides the photoinduced warming up, the laser excitation leads to the charge transfer and thus to the formation of charged species. That is why the photoinduced spectrum of EB (Fig. 4) differs from the difference spectrum of the thermally heated EB film [Fig. 3(a)]. Nevertheless, one must note the general similarity of these spectra both in the region of the absorption with a slight maximum at 400–500 nm, and in the region of the bleaching with a large broad maximum at 550–800 nm.

When the pulse energy of the photoexcitation is large enough and many excitons appear, the shells of the neighbor excitons overlap so that the electrons from the exciton shells can move in the Coulomb field of several cations placed in the center of each overlapping exciton. We believe this state to be just the electron-hole plasma (*e-h* plasma), found in the photoexcited semiconductors (see Ref. 61, and references therein). According to Refs. 61–64, the *e-h* plasma has a longer lifetime than that of the free exciton gas. The regions of the polymer sample where the *e-h* plasma appears are quasimetallic. The existence and stability of these quasimetallic regions can be substantiated by the photoinduced-conductivity measurements performed on EB.[4,9,12] The conjugated fragments of the polymer chains (CF's), which accommodate the *e-h* plasma electrons, do not contribute to the absorption spectrum of the nonexcited polymer because these CF's absorb in another spectral region. That is why the bleaching is observed where the maximum was before. The intensity of the bleaching is proportional to the fraction of the sample volume occupied by the *e-h* plasma. The regions of the polymer sample occupied by the exciton gas also do not contribute to the polymer absorption spectrum and should also lead to the bleaching effect. The effect of the exciton gas and of the *e-h* plasma on the optical absorption has been discussed for semiconductor quantum-well structures.[62,63]

The similar effect of the UV-spectrum bleaching can be observed for conducting polymers upon doping. The typical examples can be found in the review by Patil, Heeger, and Wudl[65] We attribute the effect of the broad maximum bleaching in this case to the formation of the Coulomb impurity centers (CIC's) in the polymer upon doping.[19,20] A charged impurity is located in the middle of the CIC, and the charge of the opposite sign is delocalized over 10–30 CF's environing the impurity. These fragments form the CIC shell. The CIC absorbs in the IR region; the CF's from the CIC shell do not contribute to the absorption of the pristine polymer in the UV region. The increase of the dopant concentration enhances the absorption in the IR region, which is the CIC's own absorption. The absorption characteristic for the pristine polymer decreases (see examples in Ref. 65).

The effect of the photoexcitation on conducting polymers can be treated as photodoping, which creates the regions containing either the *e-h* plasma (the CF-cation's congestion is able to accommodate many electrons) or the exciton gas. The formation of the separate Coulomb impurity centers (it may be either a CF cation, or a CF anion or another charged impurity) having electrons (or holes) on the CF's in its proximity is also possible. Below we shall discuss our experimental data from the point of view of these concepts.

Very soon (about some ps) after the photoexcitation many CF cations are formed. They can be detected by the absorption spectroscopy since the neutral and positively charged CF's have absorption maxima in various parts of the spectrum. Actually, the absorption of EB is stronger than that of ES in the region ranging from 500 to 700 nm and weaker than that of ES for $\lambda > 700$ nm (see Fig. 2). It is known that after the doping of the aniline tetramers of LB and EB types with I_2 and HCl the positively charged tetramers appear. At the same time the absorption decreases in the region from 500 to 700 nm and increases for $\lambda > 700$ nm as compared to the spectrum of the undoped tetramer.[37] Based on these data we attribute the difference in the spectra of absorption of EB and ES polymers to the difference in absorption of neutral and charged CF's.

The polymer photodoping concept is also confirmed by the analysis of the $\Delta D_{\rm ph}(t)$ dependence at various values of the pulse energy. First of all we must note that the formation of charged species due to the absorption of a single quantum ($\simeq 2$ eV, $\lambda = 590$ nm) is permitted by relation (1) (see also Sec. IV B). It explains the linear relation

of ΔD_{ph} to P at 555 and 660 nm for $P<2$ mJ/cm^2 and $\tau=0$ (see Fig. 5). Roe *et al.*[11] have also fixed the linear relation of ΔD_{ph} to P ($\hbar w \simeq 2$ eV, $P \leq 10^{-3}$ mJ/cm^2) for EB. Phillips *et al.*[12] have noticed the linear increase of the photocurrent with P in this material.

At $P=2$ mJ/cm^2 the full energy absorbed in the sample corresponds approximately to one absorbed quantum per one aniline tetramer. In the case of a many-quantum formation of cations (CF^{2+}, CF^{4+}, and so on), a stronger dependence of ΔD_{ph} on P, type P^n, $n>1$, should be observed. The multicharged cations (which apparently exist in the salt upon doping of emeraldine by I_2 or HCl) appear upon photodoping due to some charge-transfer processes taking place in the system in the very moment of irradiation and immediately after it is cut out. At present it is impossible to estimate theoretically the yield of the various charged products as a function of P. The complexity of the problem becomes apparent when one notices that for the different domains of the photoinduced spectrum the different functional form of the ΔD_{ph} dependence on P has been found:[7] $\Delta D_{ph} \simeq P^{1/2}$ in the region 0.9–1.4 eV and $\Delta D_{ph} \simeq P$ in the region 1.8 eV. Here we limit our considerations on presenting the arguments in favor of the relation $\Delta D_{ph} \simeq P^n$, $n \neq 1$.

Deviation from the linear dependence of $\Delta D_{ph} \simeq P$ for $P>2$ mJ/cm^2 and $\tau=0$ (Fig. 5) may be caused by the increase of the probability of the two-quantum ionization processes. The rates of the recombination processes are proportional to the concentrations of all the recombinating particles. This should change the power n in the relation $\Delta D_{ph} \simeq P^n$ in a complicated manner. Relations $\Delta D_{ph} \simeq P^n$ with various $n \simeq 1$ and $n \simeq \frac{1}{2}$ for the different regions of the photoinduced spectrum[7] provide evidence that this spectrum is a superposition of various contributions. The observed increase of ΔD_{ph} with the increase of P at 660 nm ($\tau=600$ ps) and at 555 nm ($\tau=300$ ps) (Fig. 5) is caused by the growth of the region occupied by the *e-h* plasma. The difference in the values of ΔD_{ph} for $\tau=0$ and $\tau=300$ ps [Fig. 5(a)] and $\tau=0$ and $\tau=600$ ps [Fig. 5(b)] proves the complexity of the kinetic processes occurring in the system after the photoexcitation.

At low pulse energy ($\hbar w \simeq 2$ eV, $P<10^{-3}$ mJ/cm^2) Roe *et al.*[11] obtained that (i) the maximum value of ΔD_{ph} was 2×10^{-3}, and (ii) a good fit to their data was

$$\Delta D_{ph} \simeq A \exp(-t/\tau_1)+B \exp(-t/\tau_2)+C$$

with $\tau_1=30$ ps, $\tau_2=600$ ps, $B/A=0.5$, and $C/A=1.14$. Perhaps this formula, rejected in Ref. 11 as a very complex one, takes into account some sort of the contributions ($A,B,C,\ldots$) from different species to the bleaching. We think that the values of A,B,C are expected to be different functions of P. At the high pumping energy, $P \simeq 1$ mJ/cm^2, we also observe a slow component which manifests in the small decrease of the bleaching in the region from 540 to 720 nm in 500 ps [Figs. 4(a) and 4(b)] and the rapid (in 100 ps) components describing the decrease of bleaching [Figs. 6(a) and 7(a)] followed by a plateau with ΔD_{ph} constant in the ps range. We think that the rapid component of photobleaching [Figs. 6(a) and 7(a), $\tau \leq 100$ ps] appears due to relaxation of separate excitons and pairs of cations and electrons, which are formed near each other (the CF cations in this spectral region are absorbed weaker than the neutral CF's), and the plateau [Figs. 6(a) and 7(a), $\tau>100$ ps] appears due to formation of the regions with the steady *e-h* plasma and Coulomb impurity centers (CF's from regions having *e-h* plasma and the Coulomb impurity centers do not contribute to the EB absorption spectrum, leading to the bleaching). The part with a rapid decrease of bleaching in Figs. 6(d) and 7(b) is absent as the pumping energy increases to $P=5$ and 10 mJ/cm^2. Under these conditions the volume of regions with the *e-h* plasma and CIC grows, and the rapid relaxation of excitons, cations, and electrons is not seen against the background of the strong bleaching due to the plasma regions. A minor increase of bleaching in the spectral region of 700 nm after 500 ps [Figs. 4(c) and 4(d)] may be connected with a more uniform film warming up which leads to bleaching in this part of spectrum. A minor decrease of the bleaching from 550 to 730 nm after 500 ps [Figs. 4(a) and 4(b)] may be connected with a certain relaxation of charged states formed by photodoping.

For $\lambda_{probe}=1066$ nm at the small pulse energy [$P=1$ mJ/cm^2, Fig. 8(a)] we observe only the rapid decline of the photoabsorption in 100 ps followed by leveling off with $\Delta D_{ph}(t) \simeq 0$. When the pulse energy increases ten times [Fig. 8(b)], the additional absorption ΔD_{ph} (which at $\tau=0$ is only 1.6 times higher than for $P=1$ mJ/cm^2) is subject to a similar rapid decrease to zero and transfers to the bleaching plateau in approximately 150–300 ps. The rapid component ΔD_{ph}, as it has been mentioned above, appears due to a considerable number of CF cations. In this spectral region they have higher absorption than the initial polymer. At the same time, their recombination with either nearly localized or having high mobility electrons is fast. We attribute the bleaching plateau in the ps range to the polymer photodoping, leading to the formation of regions with the stable *e-h* plasma and to the Coulomb impurity centers which cause the bleaching of the nonexcited polymer absorption spectrum. The contribution from the thermal warming up giving rise to the bleaching in this spectral region is also possible.

We suppose that the long (several minutes) relaxation time of the photoexcited EB to the initial state, observed in the absorption measurements, results from the processes in the polymer material as an integral entity rather than in a separate polymer chain. The charged states formed under the laser pulse play the main role in these processes. We have not made the quantitative estimates of the photostimulated warming-up contribution to the differential spectra changes, though the effect of warming up, as it was mentioned above, is considerable. We must note that the relaxation of the charged states becomes slower if the film, heated upon photoexcitation, is cooled, the heat being lost through the film surface during some sufficiently macroscopic time (seconds or minutes). Besides, the thermal heating may accompany the relaxation of the charged states, since each act of the charge recombination (electrons with CF cations) and the relaxation of an exciton excitation releases the energy of $\simeq 2$ eV which is not irradiated but is transformed mainly into the heat.

That is why the local heating contributes to the changes of differential spectra during all the period of relaxation of excited and charged states. The contribution to ΔD from the variation of the dielectric constant[58] due to the appearance of charged species cannot be eliminated; for example, it is well known that the changes of the dielectric constant are considerable if EB transforms into ES.[22]

In the literature, the long relaxation times of the PANi photoinduced spectra are usually associated with hindered ring rotations which create considerable obstacles for the movement of the charged defects created in a chain after photoexcitation.[5,6,11–15] Since the early 1980s, concepts of theoretical physics, including solitons, polarons, and bipolarons have been applied to conjugated polymers.[66,67] Many of the properties of conducting polymers are usually described in terms of these states.[66–69] The charged defects in polyacetylene and polythiophene have been shown to have low masses, large electron-phonon coupling, and relatively low pinning. Similar consideration of the experimental results for polyaniline demonstrated the important role of polarons with large mass, strong pinning, and low mobility in this system.[6] However, we would like to draw attention to certain limitations and difficulties in the utilization of the above concepts.

First, the long polyacetylene chain is an alternant hydrocarbon molecule, and, due to the pairing theorem,[70] any carbon atom of the chain has exactly one π electron in any (ground or excited) state. This conclusion of the pairing theorem is unaffected by the bond-length distortions keeping up the conjugation. In accord with this theorem, no electron-phonon excitation in the polyene chain can give rise to the localized and separated charges of a bipolaron type. Thus, it follows that the conjecture stating that photoinjection of an *e-h* pair on a polymer chain leads to its fast thermalization with subsequent conversion to a pair of charged topological defects, i.e., to a soliton-antisoliton pair,[71] contradicts the pairing theorem for conjugated molecules. The conclusions of the pairing theorem are correct in general also for PANi although the presence of nitrogen atoms slightly violates the pairing theorem conditions. After the electronic excitation, the slight changes of electronic density on chain atoms are possible. However, these changes for low-energy excitations should not give rise to an appreciable charge separation within a single chain.

The second point is the vanishing of the current density for an electron in a one-dimensional conjugated chain,[72] and the impossibility to account for charge transport along a chain in the framework of quantum mechanics. The diffusionlike movement of an electron along a chain or any relaxation process with an electron transfer along a chain requires many states, separated or slightly interacting, which are successively placed along a chain. But the conjugated fragment has only the states delocalized throughout the entire chain. Thus the conjugated fragments of polymer chains are not metallic (see also any discussion in Ref. 73). A separate polymer chain (as well as a separate fragment of the chain) cannot be treated as a conducting (metallic) molecular wire. This chain (or fragment) with respect to external influence always behaves as an integral entity and is a basic structural unit of a polymer material. Recently, this notion was experimentally supported for polypyrrole chains isolated within the channels of zeolites.[74] The fully oxidized chain does not exhibit, inside the zeolite, metallic ac conductivity, although they are conducting in a bulk polymer. NMR experiments[75,76] have also demonstrated the absence of movement of any defects in polyene chains. So the *only possibility* for creating charged species and conducting states in conducting polymers is the electron transfer between adjacent chains or their fragments.

A simple idea that in quasi-one-dimensional systems the conductivity is governed by electron hops between fragments has been discussed.[46,77,78] For example, in this case, the anisotropy of conductivity ($\sigma_{\parallel}/\sigma_{\perp}$) is governed by the ratio of the diffusion coefficients along different directions: $\sigma_{\parallel}/\sigma_{\perp} \cong D_{\parallel}/D_{\perp}$. The diffusion coefficients ($D_{\parallel}$ and $D_{\perp}$) themselves are proportional to the squares of the displacements of an electron along different directions as a result of one hop. In one hop along a square lattice of fragments an electron travels a distance of about $L/2$ along the chain axes direction and d along the perpendicular direction. Consequently, one finds $\sigma_{\parallel}/\sigma_{\perp} \cong (L/2d)^2$ in fair agreement with the experimental data (see Refs. 46 and 77, and references therein). As noted in this paper, there are regions where the electrons move *coherently* over fragments (excitons and Coulomb impurity centers). In this case, the conductivity is apparently governed by the hops of electrons between these quasimetallic regions, an anisotropy of which will maintain approximately the same the conductivity anisotropy. So it appears that the interchain hopping is only the first stage in the understanding of electron transport in conducting polymers.

V. CONCLUSIONS

The results of the spectral and kinetic (in ps range) studies of the emeraldine base in the high-intensity pulse laser field are described within the new approach to conducting polymers, which has been earlier developed and used for the interpretation of electrophysical properties of polyacetylene. This approach is based on the observation that in the "real" polymer material the polymer chain is always broken by the chain defects into conjugated fragments of a finite length. In this case, the neighbor fragments of the neighboring chains are connected by the resonance interaction, and the corresponding parameter of the electron hopping is about 0.1 eV. As a result, the conducting polymer should be treated as a 3D system of the long conjugated fragments. Within this model, the electrophysical characteristics of the conducting polymer are determined by rather general characteristics of electronic structure of the conjugated fragments and much more by their mutual arrangement in the polymer material, which governs the magnitude of the electron interfragment hopping and the electronic polarization of the other fragments, surrounding the charged fragment (or the dopant). From this point of view, the similarity of the electric properties of various conducting polymers be-

comes comprehensible: it is a consequence of the proximity of the principal characteristics of the conjugated fragments of various polymers. No matter what the peculiarities of the inner structure and chemical composition of the conjugated fragment are, its ionization potential is always ca. 6 eV, its electron affinity is $\simeq 1$ eV, the energy of the first π electron excitation is $\simeq 2$ eV, and the electrostatic energies of the interaction between a charged species and the surrounding medium in conducting polymer, i.e., the polarization energy, is $\simeq 1.5$ eV.

We were able to explain metallic conductivity in the emeraldine salt and the appearance of charged species in the emeraldine base in the concentration proportional to the pumping power, after absorption of just one photon with an energy of $\simeq 2$ eV, that is to account for the linear relation of photoinduced excitation to the exciting pulse intensity. We think that our explanation of the slow component in the photoinduced electron spectra of the emeraldine base in terms of charged fragments is more realistic than that invoking long isolated chains and large twists of the rings in the polyaniline polymer chains. Moreover, these twists in the polymer materials seem to be hindered, and their existence is not confirmed by experimental data. Having considered the physical processes in polyaniline from the point of view of the fragment model of the polymer material, we suggest that other experiments, usually considered as those supporting the models based on the peculiarities of the structure of isolated polymer chains of conducting polymers, can be reinterpreted. It seems that we gave the convincing evidence in favor of the polyaniline three-dimensional fragment model, which naturally requires further development for more detailed description of experimental data.

ACKNOWLEDGMENTS

The authors are grateful to Dr. A. L. Tchougreeff for his valuable discussions and help in the preparation of the manuscript and to Dr. A. N. Shchegolikhin for the measurements with a Perkin-Elmer spectrometer. The work of I.A.M. was supported, in part, by a Soros Foundation Grant awarded by the American Physical Society. T.S.Z. and V.M.G. thank the ELORMA company for financial support.

[1] *Proceedings of the International Conference on Synthetic Metals* [Synth. Met. **27** (1988); **28** (1989); **29** (1989)] [Synth. Met. **41-43** (1991)].

[2] Y. H. Kim, C. Foster, J. Chiang, and A. J. Heeger, Synth. Met. **26**, 49 (1988).

[3] Y. H. Kim, C. Foster, J. Chiang, and A. J. Heeger, Synth. Met. **29**, E285 (1989).

[4] R. P. McCall, M. G. Roe, J. M. Ginder, T. Kusumoto, A. J. Epstein, G. E. Asturias, E. M. Scherr, and A. G. MacDiarmid, Synth. Met. **29**, E433 (1989).

[5] R. P. McCall, J. M. Ginder, J. M. Leng, H. J. Ye, S. K. Manohar, J. G. Masters, G. E. Asturias, A. G. MacDiarmid, and A. J. Epstein, Phys. Rev. B **41**, 5220 (1990).

[6] R. P. McCall, J. M. Ginder, M. G. Roe, G. E. Asturias, E. M. Scherr, A. G. MacDiarmid, and A. J. Epstein, Phys. Rev. B **39**, 10 174 (1989).

[7] M. G. Roe, J. M. Ginder, P. E. Wigen, A. J. Epstein, M. Angelopoulos, and A. G. MacDiarmid, Phys. Rev. Lett. **60**, 2789 (1988).

[8] M. G. Roe, J. M. Ginder, R. P. McCall, K. R. Gromack, A. J. Epstein, T. L. Gustafson, M. Angelopoulos, and A. G. MacDiarmid, Synth. Met. **29**, E425 (1989).

[9] Y. H. Kim, S. D. Phillips, M. J. Novak, D. Spiegel, C. M. Foster, G. Yu, J. C. Chiang, and A. J. Heeger, Synth. Met. **29**, E291 (1989).

[10] A. P. Monkman and P. Adams, Synth. Met. **41**, 891 (1991).

[11] M. G. Roe, J. M. Ginder, T. L. Gustafson, M. Angelopoulos, A. G. MacDiarmid, and A. J. Epstein, Phys. Rev. B **40**, 4187 (1989).

[12] S. D. Phillips, G. Yu, Y. Cao, and A. J. Heeger, Phys. Rev. B **39**, 10 702 (1989).

[13] J. M. Ginder, A. J. Epstein, and A. G. MacDiarmid, Synth. Met. **43**, 3431 (1991).

[14] R. P. McCall, J. M. Ginder, J. M. Leng, K. A. Coplin, H. J. Ye, A. J. Epstein, G. E. Asturias, S. K. Manohar, J. G. Masters, E. M. Scherr, Y. Sun, and A. G. MacDiarmid, Synth. Met. **41**, 1329 (1991).

[15] J. M. Leng, J. M. Ginder, R. P. McCall, H. J. Ye, A. J. Epstein, Y. Sun, S. K. Manohar, and A. G. MacDiarmid, Synth. Met. **41**, 1311 (1991).

[16] *Handbook of Conducting Polymers,* edited by T. A. Skotheim (Dekker, New York, 1986), Vols. 1 and 2.

[17] J. P. Pouget, in *Electronic Properties of Polymers and Related Compounds,* edited by H. Kusmany, M. Mehring, and S. Roth (Springer, Berlin, 1985), p. 24.

[18] J. P. Pouget, M. E. Jozefowicz, A. J. Epstein, X. Tang, and A. G. MacDiarmid, Macromolecules **24**, 779 (1991).

[19] I. A. Misurkin, Dokl. Akad. Nauk SSSR **296**, 1159 (1987) [Sov. Phys. Dokl. **296**, 1001 (1987/1988].

[20] I. A. Misurkin and A. Yu. Cohn, Europhys. Lett. **11**, 145 (1990).

[21] I. A. Misurkin and A. P. Frolov, Europhys. Lett. **11**, 151 (1990).

[22] Z. W. Wang, C. Li, E. M. Scherr, A. G. MacDiarmid, and A. J. Epstein, Phys. Rev. Lett. **66**, 1745 (1991).

[23] A. F. Diaz and J. A. Logan, J. Electroanal. Chem. **111**, 111 (1980).

[24] D. E. Stellvel and S. M. Park, J. Electrochem. Soc. **135**, 2491 (1988).

[25] H. Kusmany, N. S. Sacriciftci, Synth. Met. **18**, 353 (1987).

[26] A. Thyssen, A. Borgerding, and J. W. Schultze, Makromol. Chem. Macromol. Symp. **8**, 143 (1987).

[27] K. Andryunas, Yu. Vishchakas, V. Kabelka, I. V. Mochalov, A. A. Pavlyuk, G. T. Petrovskii, and V. Syrus, Pis'ma Zh. Eksp. Teor. Fiz. **42**, 333 (1985) [JETP Lett. **18**, 410 (1985)].

[28] A. P. Monkman, D. Bloor, G. C. Stevens, and J. C. H. Stevens, J. Phys. D **20**, 1337 (1987).

[29] R. J. Cushman, P. M. McManus, and S. C. Jang, J. Electroanal. Chem. **291**, 335 (1986).

[30] M. Wan, Synth. Met. **31**, 51 (1989).

[31] B. R. Weinberger, C. B. Roxlo, S. Etemad, G. L. Baker, and J. Orenstein, Phys. Rev. Lett. **53**, 86 (1984).

[32] U. Rauscher, H. Bässler, D. D. C. Bradley, and M. Hennecke, Phys. Rev. B **42**, 9830 (1990).

[33] B. Themans, J. M. André, and J. L. Bredás, in *Electronic Properties of Conducting Polymers and Related Compounds,* edited by H. Kuzmany, M. Mehring, and S. Roth (Springer, Berlin, 1985), p. 107.

[34] S. Stafström, in *Electronic Properties of Conducting Polymers and Related Compounds* (Ref. 33), p. 238.

[35]I. A. Misurkin and A. A. Ovchinnikov, Usp. Khim. **46**, 1835 (1977) [Russ. Chem. Rev. **46**, 967 (1977)].
[36]B. Sjögren and S. Stafström, J. Chem. Phys. **88**, 3840 (1988).
[37]Y. Cao, S. Li, Z. Xue, and D. Guo, Synth. Met. **16**, 305 (1986).
[38]W. M. Salaneck, C. R. Wu, S. Stafström, M. Lindgren, T. Hjertberg, O. Wennerström, M. Sandberg, C. B. Duke, E. Conwell, and A. Paton, in *Electronic Properties of Conducting Polymers and Related Compounds* (Ref. 33), p. 253.
[39]C. B. Duke, E. M. Conwell, and A. Paton, Chem. Phys. Lett. **131**, 82 (1986).
[40]M. J. S. Dewar, J. Chem. Soc. **1952**, 3532.
[41]E. M. Conwell, C. B. Duke, A. Paton, and S. Jeyadev, J. Chem. Phys. **88**, 3331 (1988).
[42]L. W. Shacklette, J. F. Wolf, S. Gould, and R. H. Baughman, J. Chem. Phys. **88**, 3955 (1988).
[43]T. Terao, S. Maeda, T. Yamabe, K. Akagi, and H. Shirakawa, Chem. Phys. Lett. **103**, 347 (1984).
[44]K. Soga and M. Nakamaru, J. Chem. Soc., Chem. Commun. **24**, 1495 (1983).
[45]A. Yu. Cohn and I. A. Misurkin, Teor. Eksp. Khim. **25**, 393 (1989) [Theor. Exp. Chem. **25**, 366 (1989)].
[46]A. L. Tchougreeff and I. A. Misurkin, Fiz. Tverd. Tela (Leningrad) **30**, 1043 (1988) [Sov. Phys. Solid State **30**, 605 (1988)].
[47]J. L. Brédas, R. Silbey, D. S. Bordeaux, and R. R. Chance, J. Am. Chem. Soc. **105**, 6555 (1983).
[48]N. Sato, K. Seki, and H. Inokuchi, J. Chem. Soc., Faraday Trans. 2 **77**, 1621 (1981). This paper gives the electrostatic energies of interaction between a charged species and surrounding medium (i.e., polarization energy) for organic molecules as determined by the difference (typically 1.5–2 eV) in gas-phase and solid-state ionization energies (Ref. 47).
[49]M. Born, Z. Phys. **79**, 62 (1932).
[50]W. Klemm, Z. Phys. **82**, 529 (1933).
[51]A. W. Overhauser, Phys. Rev. **101**, 1702 (1956).
[52]I. A. Misurkin, A. V. Soudackov, and A. Yu. Cohn (unpublished).
[53]T. C. Koopmans, Physica **1**, 104 (1933).
[54]R. de Surville, M. Josefowicz, L. T. Yu, J. Perichon, and R. Buvet, Electrochim. Acta **13**, 1451 (1968).
[55]F. Zuo, M. Angelopuolos, A. G. MacDiarmid, and A. J. Epstein, Phys. Rev. B **36**, 3475 (1987); **39**, 3570 (1989).
[56]L. Onsager, J. Am. Chem. Soc. **58**, 1486 (1936).
[57]C. J. F. Bottcher, *Theory of Electric Polarization* (Elsevier, Amsterdam, 1952).
[58]W. Liptay, in *Modern Quantum Chemistry, Istanbul Lectures,* edited by O. Sinanoğlu (Academic, New York, 1965).
[59]N. G. Bakhshiev, *Spectroscopy of Intermolecular Interactions* (Nauka, Leningrad, 1972).
[60]J. M. Ginder, K. Kim, J. M. Leng, and A. J. Epstein, Bull. Am. Phys. Soc. **35**, 419 (1990).
[61]H. Haug and F. F. Abraham, Phys. Rev. B **23**, 2960 (1981).
[62]S. Schmitt-Rink, D. S. Chemla, and D. A. B. Miller, Phys. Rev. B **32**, 6601 (1985).
[63]W. H. Knox, R. L. Fork, M. C. Downer, D. A. B. Miller, D. S. Chemla, C. V. Shank, A. C. Gossard, and W. Wiegmann, Phys. Rev. Lett. **54**, 1306 (1985).
[64]H. Kalt, K. Reimann, W. W. Rühle, M. Rinker, and E. Bauser, Phys. Rev. B **42**, 7058 (1990).
[65]A. O. Patil, A. J. Heeger, and F. Wudl, Chem. Rev. **88**, 183 (1988).
[66]A. J. Heeger, S. Kivelson, J. R. Schrieffer, and W.-P. Su, Rev. Mod. Phys. **60**, 781 (1988).
[67]A. J. Heeger, Polym. J. **17**, 201 (1985); J. L. Brédas and G. B. Street, Acc. Chem. Res. **18**, 309 (1985).
[68]E. Ehrenfreund, Z. Vardeny, O. Brafman, and B. Horovitz, Phys. Rev. B **36**, 1535 (1987); Z. Vardeny, E. Ehrenfreund, O. Brafman, A. J. Heeger, and F. Wudl, Synth. Met. **18**, 183 (1987).
[69]B. Horovitz, Solid State Commun. **41**, 729 (1982).
[70]A. D. McLachlan, Mol. Phys. **4**, 49 (1961); P. B. Visscher and L. M. Falicov, J. Chem. Phys. **52**, 4217 (1970).
[71]W.-P. Su and J. R. Schrieffer, Proc. Natl. Acad. Sci. U.S.A. **77**, 5626 (1980); M. J. Rice, Phys. Lett. **71A**, 152 (1979); I. Zozulenko, J. Phys. Condens. Matter **5**, 3611 (1993).
[72]P. W. Atkins, *Molecular Quantum Mechanics,* 2nd ed. (Oxford University Press, Oxford, 1983), p. 389.
[73]A. L. Tchougreeff and I. A. Misurkin, Il Nuovo Cimento D **14**, 833 (1992).
[74]L. Zuppiroli, F. Beuneu, J. Mory, P. Enzel, and T. Bein, Synth. Met. **57**, 5081 (1993).
[75]C. S. Yannoni and T. C. Clarke, Phys. Rev. Lett. **51**, 1191 (1983).
[76]H. Thomann, H. Lin, and G. L. Baker, Phys. Rev. Lett. **59**, 509 (1987).
[77]R. H. Baughman and L. W. Shacklette, Phys. Rev. B **39**, 5872 (1989).
[78]L. W. Shacklette and R. H. Baughman, Mol. Cryst. Liq. Cryst. **189**, 193 (1990).